Composites: Part A 184 (2024) 108258

Contents lists available at ScienceDirect

Composites Part A

journal homepage: www.elsevier.com/locate/compositesa

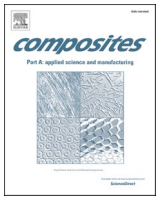

Compression and hydrothermal ageing after impact of carbon fibre reinforced epoxy laminates

Rowan L. Caldwell [a,*], Peter Davies [b], Mael Arhant [b], B. Gangadhara Prusty [a,c]

[a] ARC Training Centre for Automated Manufacture of Advanced Composites, School of Mechanical & Manufacturing Engineering, UNSW Sydney, NSW 2052, Australia
[b] Ifremer RDT, Research and Technology Development Unit, 1625 Route de Sainte-Anne, Plouzané 29280, France
[c] Australian Composites Manufacturing CRC (ACM CRC), UNSW Sydney, NSW 2052, Australia

ARTICLE INFO

Keywords:
Carbon fibre
Thermosetting resin
Damage tolerance
Impact behaviour
Moisture

ABSTRACT

This paper proposes a new methodology for the assessment of seawater ageing effects on impact-damaged composite laminates. CF/Epoxy laminates which were unimpacted, and impacted at 30 J, 60 J, and 90 J by hemispherical and conical impactors were subject to 4 months hydrothermal ageing in renewed natural seawater at 60 +/-2 °C. The majority of water uptake by impacted laminates (0.05 wt% – 0.3 wt%) occurred in the first 24 h and is believed to be held in damage cavities by capillary mechanisms. The increase in diffusive water uptake rate by the matrix due to impact damage was only small, at less than 0.008 wt%.mm.hr$^{-0,5}$, compared with the total diffusive water uptake rate of 0.1 wt%.mm.hr$^{-0,5}$. Hydrothermal ageing reduced the residual compressive strength of pristine laminates by 25 % and impact-damaged laminates by 8 % to 16 % for impacts between 30 J and 90 J.

1. Introduction

1.1. Types of ageing

Materials with polymeric constituents are vulnerable to changes in physical and mechanical properties throughout their lifetime even in the absence of load due to ageing. Polymer matrix composites exposed to marine environments are susceptible to two types of ageing: (a) physical ageing, which occurs in all composite materials under normal storage and service conditions and (b) seawater aging, which occurs during immersion [1].

Physical ageing's effect on impact performance is not often studied specifically as physical ageing occurs during most tests on composite materials as a product of normal material handling and storage. Moreover, Robin [1], who reversed physical ageing via thermal rejuvenation of CF/epoxy laminates, compared the rejuvenated laminates with physically aged laminates and found no significant difference in their impact performance. Seawater ageing however, does have a significant effect on Low Velocity Impact (LVI) performance of carbon fibre reinforced polymer composites [1] and, as such, new materials destined for marine applications still require seawater studies. Furthermore, unlike the effects of physical ageing, which are eliminated by holding at a temperature above the glass transition temperature, T_g, [2] some effects of seawater ageing are irreversible [1]. Physical changes such as increased density and volumetric swelling [3] and chemical changes, such as plasticisation, which occur during seawater ageing are considered reversible [1] while certain chemical changes such as oxidation and hydrolysis are considered irreversible. Therefore, seawater ageing must be considered in the design of marine composite structures [4].

Seawater aging is caused by moisture absorption. In composites, water molecules typically diffuse along the interface between the fibre and matrix and into microcracks [5]. This makes areas with exposed fibres, such as cut edges and impact damage sites potentially more sensitive to seawater ageing. According to Ramirez et al [6], chemical interphase degradation, in the form of reduced interfacial adhesion between fibre and matrix, can occur during seawater ageing degrading mechanical properties and increasing capillary moisture uptake. Epoxies are referred to as hydrophilic as they can absorb up to 5 % water by weight [7]. The water uptake rate depends on time, temperature, constituent materials, and interface chemistry. Therefore, over short durations, thick composite laminates may never reach a state of equilibrium absorption and assumptions about their properties based on fully-aged laminates may not be accurate. To speed up the ageing of thick materials, the increased kinetics of water absorption at higher temperatures is

* Corresponding author.
E-mail address: rowan.caldwell@unsw.edu.au (R.L. Caldwell).

https://doi.org/10.1016/j.compositesa.2024.108258
Received 21 March 2024; Received in revised form 1 May 2024; Accepted 3 May 2024
Available online 6 May 2024

leveraged to accelerate ageing effects in a process known as hydrothermal or accelerated ageing. Hydrothermal ageing is frequently used to accelerate laboratory seawater ageing tests and achieve ageing levels equivalent to several years in seawater over several months.

1.2. Role of seawater ageing on composite impact behaviour

Hydrothermal ageing is widely considered to negatively affect mechanical properties, impact resistance and residual strength of typical thermosetting polymer matrix composites [8–11]. A recent review by Fernandes et al [12] discusses seawater ageing issues for polymeric composites in the marine environment. Typically, thermoset-based composites exposed to hydrothermal ageing experience: (a) reduced elastic modulus caused by matrix plasticisation which depends on the moisture uptake, and (b) reduced mechanical strength primarily due to fibre/matrix interface degradation leading to lower residual strengths for aged then impacted laminates [13–16]. Plasticisation often results in lower peak impact forces, threshold loads and threshold energies and greater deflections and contact times [13–15,17–21]. An illustration of the typical LVI response of hydrothermally aged GFRP laminates is shown in Fig. 1a and a comparison of the post-LVI, compressive strength of GFRP laminates following 3, 6, 12, 24, and 30 months hydrothermal ageing with unaged laminates, revealing significant decreases, even after 6 months is presented in Fig. 1b.

However, not all studies agree on the effect of ageing on impact performance. For example, Imielińska and Guillaumat [22] observed insignificant changes to threshold load and energy absorption for aramid/glass reinforced epoxy laminate impacts despite the laminates absorbing approximately 4 % water by weight. Kimpara et al [23] observed no change to CAI behaviour with different water absorption levels while Dale et al [24] noticed reduced residual strengths in aged laminates despite no change in dynamic impact behaviour. Berketis et al [16] suggested that larger delamination areas due to longer immersion durations resulted in increased impact energy absorption. Abdel-Magid et al [25] observed small improvements in strength and strain at failure in GF/epoxy laminates after short immersion times and significant decreases at longer immersion times. Deniz and Karakuzu [26] also found short ageing times of up to 3 months to improve impact performance, suggesting that relaxation of manufacturing residual stresses occurring during the initial stages of ageing resulted in higher peak impact loads.

The matrix material has consistently been shown to significantly affect water uptake with Stober et al [27], Choqueuse et al [28], Selzer and Friedrich [29] and Vieille et al [21], all reporting that PEEK-based composites experience almost no change in mechanical properties compared to unaged specimens and far less moisture uptake, compared with their thermoset matrix counterparts which saw significant property losses. As diffusion in carbon and glass fibre reinforced thermoset laminates is primarily through-thickness and in the matrix, studies often approximate the diffusivity of composites with that of the pure matrix material [30]. However, as the evidence for this is based on the overwhelming majority of studies on undamaged laminates, this assumption may be inaccurate for impact-damaged laminates with exposed fibres, cavities and interfaces. Indeed, Kootsookos [19] found glass fibre interfaces to absorb more water at saturation than carbon when comparing CF and GF reinforced polyester and vinyl ester and suggested the effect may be the result of the sizing at the fibre–matrix interface.

Clearly, the fibre–matrix interface is a determining factor in the degrading effects of hydrothermal ageing and residual strength reduction of aged composite laminates and increasing the exposure of the fibre–matrix interface to moisture via impact damage is likely to accelerate and worsen ageing degradation. Furthermore, in the case of moisture-sealed marine laminates, with a waterproof coating, seawater ageing does not begin until the coating is penetrated by a LVI event and does not occur across the laminate face but rather only at the impact damage site. The ageing environment is then limited to post-impact ageing and does not involve the more commonly studied age-then-impact scenario. To the best of the authors knowledge only one other study, by Zhang et al [31], has investigated the effect of hydrothermal ageing on impact-damaged composite laminates and the assessment of residual strength was limited to tension-after-impact test leaving the compression-after-impact performance uncharacterised. Rubio-Gonzalez [32] also investigated ageing in GF/epoxy laminates subject to artificial damage (drilled holes) but found no influence on moisture content or diffusion rate. Therefore, the following key research question remains unanswered: Does exposing fibres via LVI accelerate post-impact hydrothermal ageing rates and does this amplify the reduction in residual strength?

2. Methods

This work evaluates the effect of post-impact ageing, rather than the more commonly investigated post-ageing impact, on residual compressive strength of laminates. A new methodology titled “compression-after-ageing-after-impact” (CAAAI), is established to characterise the effect of LVI damage and subsequent hydrothermal ageing on the residual compressive strength of polymer matrix composites. The range of impact scenarios considered includes impacts at energy levels of 30 J, 60 J and 90 J by hemispherical impactors and conical impactors on 4.4

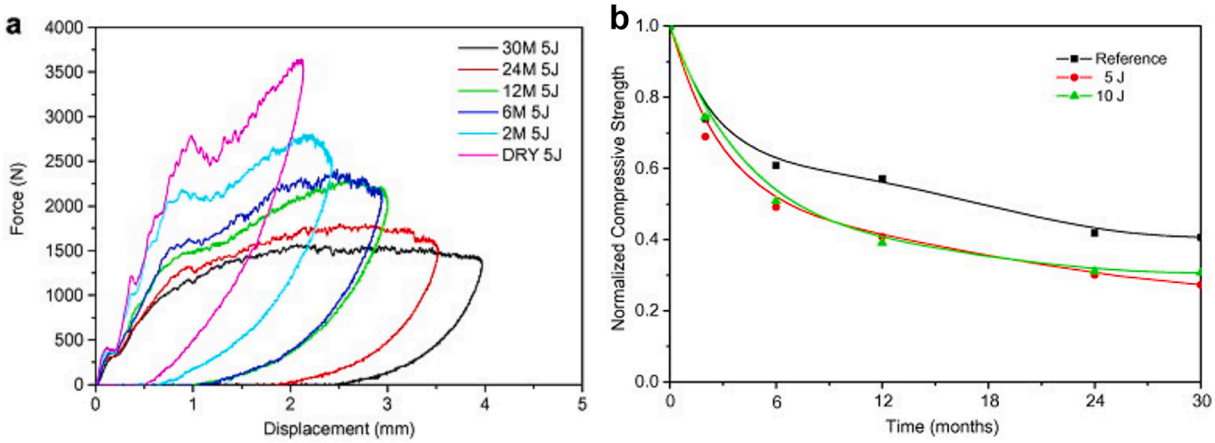

Fig. 1. (a) Typical force–displacement response for GFRP laminates impacted at 5 J after various water immersion times between zero and 30 months [16] and (b) normalised compressive strength for the same GFRP laminates following 5 J and 10 J impacts and no impact [16](Reprinted from Materials & Design, Vol 29, K. Berketis,D. Tzetzis,P.J. Hogg, The influence of long term water immersion ageing on impact damage behaviour and residual compression strength of glass fibre reinforced polymer (GFRP), Page 1300–1310, Copyright Elsevier (2024), with permission from Elsevier.).

mm thick CF/Epoxy laminates. Aged and unaged laminates labelled "None, 0 J" were not impacted and represent the baseline result for the compression tests. Half of the specimens were aged and the other half were not. For both sets, aged and unaged, nine of each were impacted by a traditional, hemispherical impactor ("HS"), 9 by a conical impactor ("Con") and 3 were not impacted at all ("None"). Of each set of 9 impacted coupons, three were impacted at 30 J, three at 60 J and three at 90 J. Each individual test was repeated 3 times giving a total of 42 coupons. All tests and coupons are listed in Table 1.

The CF/epoxy laminates were manufactured at the French Research Institute for Exploitation of the Sea (IFREMER), Brest, France in large panels comprised of 8 plies of 600 g/m^2 UD T700 12 k carbon fibre with PET stitching. The plies were arranged manually in a $[+45,0,-45,90]_s$ stacking sequence and infused with a SR8100 epoxy resin and SD4772 hardener system from Sicomin. Water jet cutting was used to cut the panels into 150 x 100 mm^2 coupons and the edges were sanded flat to ensure parallel loading during CAI tests. A 3-step cure, employed by Robin [1], and [33] involving a 24 h room temperature (20 °C) cure, 16 h, 60 °C post-cure and final secondary post-cure for 2 h at 120 °C was used to ensure complete curing as recent studies have shown incomplete curing to affect water ingress [33]. The fibre volume fraction of the cured laminate was approximately 64 % and the T_g was 75 °C.

A drop weight impact system (CEAST9350) from Instron (Fig. 2c) with a drop weight of 15.392 kg was used to conduct low velocity impacts at UNSW, Sydney, Australia. The mass was dropped from different heights to give impact velocities of 1.96 m.s^{-1}, 2.78 m.s^{-1}, and 3.41 m.s^{-1} corresponding to impact energies of 30 J, 60 J and 90 J respectively. The energy range was selected to generate a range of damage scenarios between BVID and the most severe damage without perforation. The hemispherical and conical tips shown in Fig. 2a and Fig. 2b had tip diameters of 16 mm and 12.7 mm respectively and were used to compare the effect of sharp and blunt impactor damage on ageing and residual strength. Coupons were impacted centrally and in the same orientation as they were infused. Force-time data was recorded during impacts and double-integrated to determine the impactor displacement and energy absorption during the impacts. Peak force, peak displacement, peak energy absorption, contact duration and the energy permanently absorbed by the laminate were calculated.

Ultrasonic C-scanning was employed to compare internal projected damage areas of the impacted coupons. The scanning setup is pictured in Fig. 3b. Coupons were scanned nine at a time in the submerged polymer frame which rested on the stainless-steel backing plate. The scanner was controlled by an electronic control system which moved the 5 MHz probe in a raster scan motion across the coupons and recorded positional information. The ultrasonic data was acquired by the Sonatest Prisma™ system and processed to reveal the cumulative through-thickness damage areas.

Seawater ageing was conducted at IFREMER, Brest, France over a period of 4 months in a hydrothermal ageing tank (Fig. 3b) which was filled with natural, renewed seawater and heated to 60 °C to accelerate the ageing rate. The coupons were exposed to the water on all 6 sides to maintain consistency with similar ageing experiments by Robin {Robin, 2023 #196}. A temperature of 60 °C (±2°C) was selected as the maximum ageing temperature to avoid chemical changes associated with the glass-transition temperature of 75 °C. A selection of coupons, marked "B", were removed from the tank periodically (approximately every seven days) to be weighed. Excess water was drained from the coupons before they were 'patted' dry on each side and all edges using paper towel. Each coupon was then tapped on the bench again on each edge to shake out water from the surface and again patted dry with paper towel. Weight measurements were then taken using a scale with 0.1 mg accuracy before the coupons were returned to the ageing tank.

The relative percentage mass increase, M(t) was calculated using equation (1) [1] at each measurement interval where, m_t is the mass at time, t and m_0 is the dry mass of the coupon. M(t) was plotted against a time scale normalised for the individual thicknesses of each coupon by taking the square root of time and dividing by the coupon thickness giving units of hr$^{0.5}$.mm^{-1}. When the change in mass between sequential weighing intervals reached zero, the specimens were assumed to be saturated.

$$M(t) = \frac{m_t - m_0}{m_0} \tag{1}$$

Compression after impact (CAI) testing was conducted on all 42 coupons using an Instron 5585 uniaxial loading machine with a 200kN load cell. The coupons were tested on the same day they were removed from the ageing tank, limiting the average time for reversible effects to take place to about 3 h. The testing was conducted according to the ASTM D7137 standard including a 450 N preload to ensure correct fitting and contact of specimen with the jig. The compressive load was applied at a rate of 1 mm.min^{-1} until failure. Failure was determined by a drop in compressive force of more than 30 %.

3. Results and discussion

3.1. Impact response

Key impact response characteristics are plotted in Fig. 4 including peak impact force, contact time, absorbed energy and peak impactor displacement for each of the impacts by hemispherical and conical

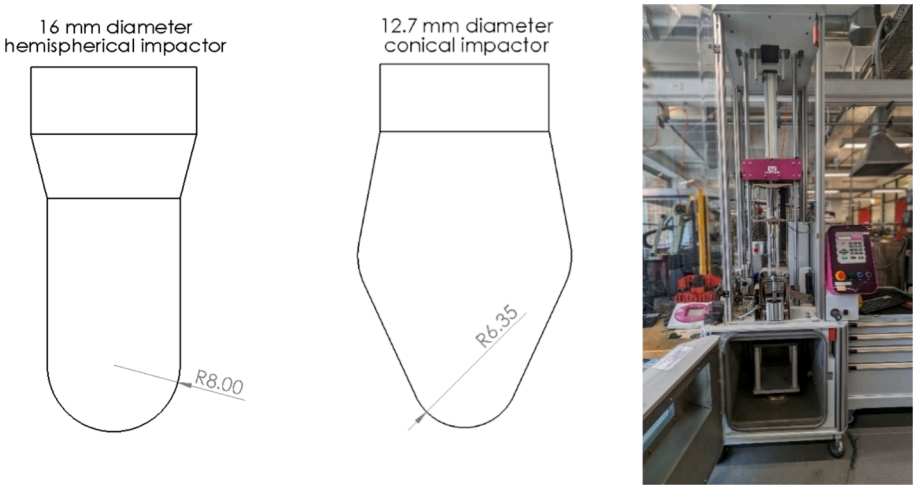

Fig. 2. (A) 16 mm diameter hemispherical impactor, (B) 12.7 mm diameter conical impactor and (C) Instron CEAST9350 drop weight impact tower.

Fig. 3. (a) Hydrothermal seawater ageing tank showing specimen removal for weighing and (b) Ultrasonic C-scanning setup showing vertical probe with transducer.

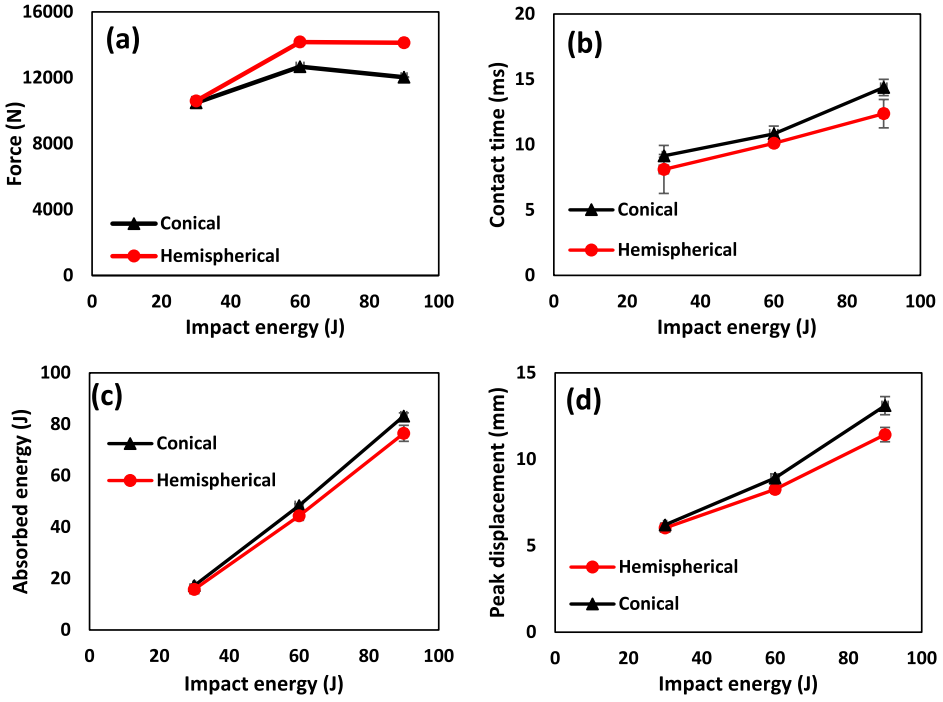

Fig. 4. Impact results for 30 J, 60 J, and 90 J impacts by hemispherical and conical impactors showing (a) peak force, (b) contact time, (c) absorbed energy, and (d) peak displacement.

impacts at the three energy levels. Raw force–time data for the impacts are not provided as the present study is focussed on ageing and residual strength and not the impacts themselves. Ultrasonic C-scan images of a sample of coupons covering the full range of impact scenarios are given in Fig. 5. The remainder of the C-scans, of an otherwise identical set of coupons subject the same impact scenarios, are given in supplementary

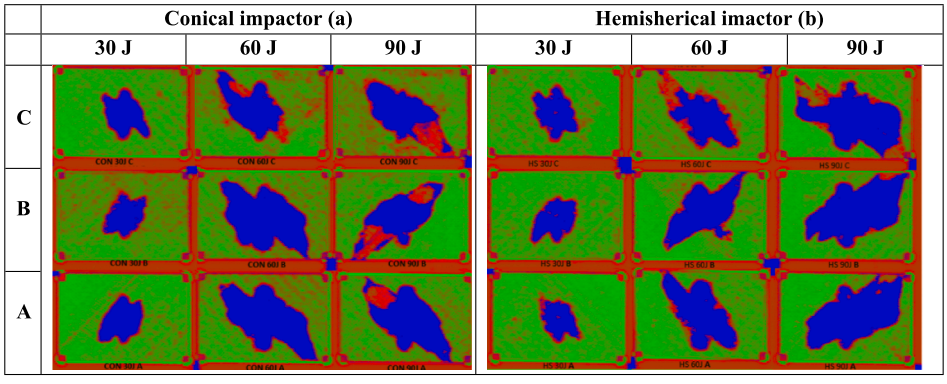

Fig. 5. Ultrasonic scan images of CF/Epoxy coupons impacted by conical impactors (a) and hemispherical impactors (b) at 30 J, 60 J and 90 J.

data (Fig. 17, Fig. 18, Fig. 19, and Fig. 20). Absorbed energy increased almost linearly with impact energy for both impactor types (Fig. 4c). Contact time (Fig. 4b) and peak displacements (Fig. 4d) revealed similar trends. Increased energy absorption, plate deflection and impact durations are related to stiffness degradation and damage. Accordingly, projected damage areas were seen to increase from 2290 mm^2 at 30 J to 4770 mm^2 at 60 J and 6820 mm^2 at 90 J, increases of around 200 % and 300 % respectively (Fig. 6a).

Conical impacts did not exhibit an entirely linear increase in impact duration and plate deflection with impact energy as stiffness degradation increased at a greater rate beyond 60 J. This is reflected in the decreased peak load (Fig. 4a) for 90 J conical impacts and projected damage areas which increased to, and plateaued beyond, 60 J, as illustrated in Fig. 6a. This is likely due to the damage approaching a delamination area limit around 60 J (Fig. 5a) and a transition to through-thickness damage penetration and back-face tow debonding. Visible matrix cracking was greater than for 90 J hemispherical impacts as illustrated in Fig. 6b and c though microscopy is required to determine the true extent of internal intralaminar damage. Compared to hemispherical impactors, conical impactors also generated deeper indentations, particularly at higher impact energies. Absorbed energies for conical impacts did not depart significantly from the hemispherical impact values as the decrease in energy absorption due to reduced delamination was countered by increased intralaminar damage due to penetration.

Peak force also increased with impact energy until extensive damage occurred beyond 60 J where the load carrying ability of laminates plateaued following hemispherical impacts and decreased following conical impacts. The plateau is believed to be due to delaminations reaching the edge of the coupons as seen in Fig. 5b. The decrease between 60 J and 90 J for conical impacts is attributed to increased penetration, fibre breakage (Fig. 7c and d) and back-face tow debonding (Fig. 7a and b). Peak force appears to show the greatest sensitivity to the changes in damage mode which result from changes in impactor and incident energy. Projected damage areas revealed low sensitivity to impactor tip geometry at 30 J and 60 J. However, more severe, 90 J impacts revealed 28 % larger damage areas (Fig. 6a) due to greater load transfer enabled by the hemispherical impactor.

3.2. Ageing

3.2.1. Water uptake in undamaged laminates

The coupons were considered saturated at the point where the unimpacted coupon reached a relative mass increase of 0.85 %, as proposed by Robin [1], who conducted a similar ageing study on the same material with the same FVF, also in 60 °C seawater. Likewise, it may be assumed that the otherwise identical, impacted coupons were also fully saturated. Saturation occurred after almost 4 months submersion at 60 °C. Mass increases (Fig. 8) beyond this time are likely the

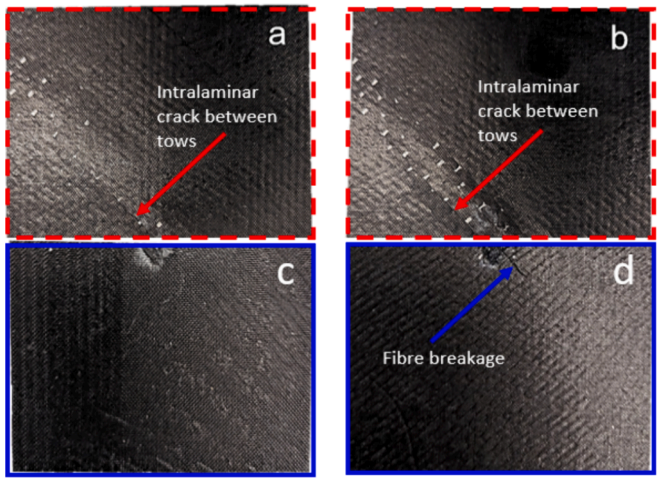

Fig. 7. Back-face impact damage due to 60 J (a) and 90 J (b) impacts by a conical impactor showing greater back-face tow debonding and intralaminar damage at 90 J, and impact-face images of laminates impacted at 60 J (c) and 90 J (d) by the conical impactor. Blue arrow indicates fibre breakage.

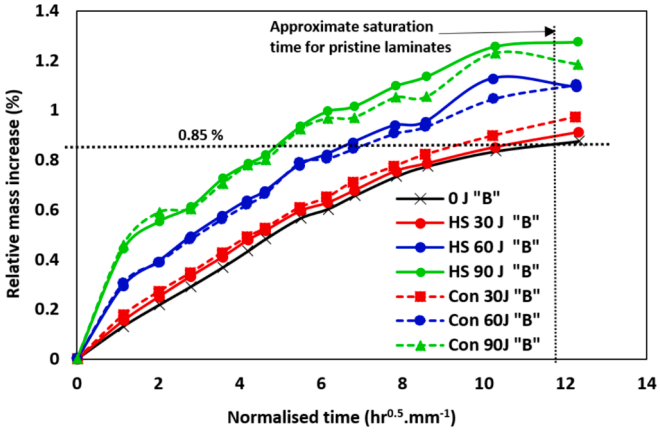

Fig. 8. Percentage mass increase via water uptake during hydrothermal ageing at 60 °C of CF/Epoxy coupons impacted by a conical (Con) impactor and a hemispherical (HS) impactor.

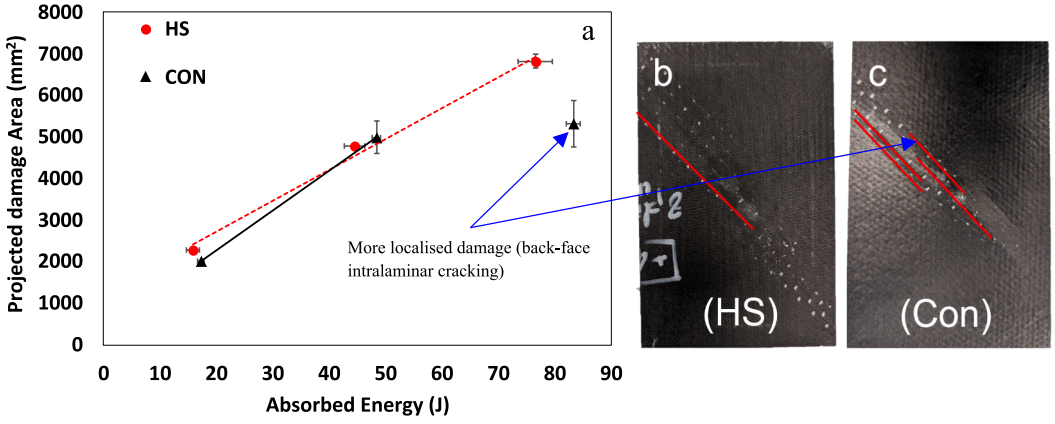

Fig. 6. (a) plot of the change in projected damage areas with impact energy and images showing back-face tow de-bonding on hemispherical (b) and conical (c) impacted coupons. Cracks between tows are delineated with red lines.

result of chemical degradation at elevated temperature as suggested by Robin [1] who found continued mass uptake at 60 °C and not at lower temperatures.

The ageing rate of the unimpacted coupons may be used to calculate the diffusivity of the composite material itself to verify the water uptake results. Taking the maximum mass uptake percentage, M_∞ of the unimpacted coupons (0 J "B") to be 0.85 % [1] and making the simplification of equation (2) [34] made by Robin [1] for isotropic diffusion in plates, equation (3) was used to calculate the diffusion coefficient for the unimpacted laminate using the linear part of the plot of 16 $t/\pi h^2$ against $M(t)/M_\infty$. A diffusivity, D of $8.00e^{-7}$ $mm^2\ s^{-1}$ was calculated from the slope of the initial linear region of the curve in Fig. 15. The value is similar to the value of $6.08e^{-7}$ $mm^2\ s^{-1}$ found by Robin [1].

$$\frac{M(t)}{M_\infty} = 1 - \frac{8}{\pi^2}\sum_i \frac{1}{(2i+1)^2} exp\left(\frac{-D(2i+1)^2\pi^2 t}{h^2}\right) \quad (2)$$

$$D = \frac{\pi h^2}{16t}\left(\frac{M(t)}{M_\infty}\right)^2 \quad (3)$$

3.2.2. Water uptake in impact damaged laminates

Water uptake in damaged laminates occurs via three main mechanisms: regular matrix diffusion via the laminate surfaces, matrix diffusion via new surface areas and fibre–matrix interfaces exposed to water by the impact damage, and water ingress into open cavities in the damage region mostly via capillary action. The schematic in Fig. 9 illustrates these three water uptake modes.

3.2.2.1. Cavity filling versus diffusion in damaged laminates. Comparing water uptake rates in Fig. 8, it is clear that more severe impact damage led to much faster initial rates of water uptake during the first 24 h (0.0–1.2 $hr^{0.5}.mm^{-1}$) of immersion. This is likely due to water ingress into small impact damage-induced cavities such as delaminations and intralaminar matrix cracks via cracks on the coupon front and back-face. This also includes uptake via the coupon edges in coupons with impact damage extending to the edges. It is expected that these coupons will see accelerated water uptake rates due to the additional fluid entry points but the total water uptake would be similar in both cases where the total damage areas are similar. Filling of these cavities relies on capillary action which is much faster than diffusion and therefore contributes far more significantly to water uptake in the first 24 h. This assumption helps explain the large initial mass increase in a short of time observed in damaged, but not undamaged laminates. Following the initial 24 h, the water uptake rates of the damaged specimens reduce to rates similar to that in the unimpacted laminate, for approximately the next 600-hour period. This suggests that, in the first 24 h, water uptake is dominated by capillary mechanisms, and, after the first 4 h, water uptake is dominated by diffusion.

While capillary flow of water and contaminants into damage-induced cavities may affect residual strength, particularly in the case of crystallisation of salt in seawater upon evaporation, these effects are presumed less consistent and more difficult to characterise. Therefore, diffusive water uptake by the matrix and its effect on residual strength, which are far more widely studied, are the focus of the investigation of residual compressive strength.

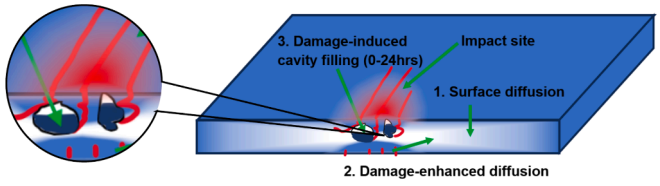

Fig. 9. Schematic showing the laminate impact site and three types of water uptake: 1. regular surface diffusion via the undamaged laminate surface, 2. diffusion from new surface areas exposed by impact damage, and 3. filling of cavities generated by impact damage.

It is not possible to directly measure the relative amount of diffusive water uptake due to new damage surfaces (labelled '2′ in Fig. 9) and the water ingress into damage cavities (labelled '3′ in Fig. 9) using present data. However, by assuming that cavity filling has reached its maximum level within the first 24 h, the diffusive water uptake rates of impacted and unimpacted laminates beyond 24 h may be compared to find the contribution of newly created damage surfaces to the diffusion rate. Indeed, the diffusive water uptake rates may be determined from the linear regions of the relative mass increase plot in Fig. 8. A select result from Fig. 8 is replotted in Fig. 10 with trendlines as an example. The plot was limited to the bilinear region (<600 hrs) for simplicity of presentation in Fig. 10. Fig. 11a compares the relative rates of surface diffusion and impact damage-induced diffusion over the 24–600 hr period. It shows that impact damage contributes a small, yet significant, fraction of the diffusion rate of water in the damaged laminates and this fraction increases with increasing damage. The relative water uptake rates, in the first 24 h and 24 to 600 h, and due to surface diffusion alone, excluding damage-induced uptake, are compared in Fig. 11b for unimpacted and hemispherical impacted laminates. Results for conical impacted laminates are not included as they were very similar to the hemispherical impactor results. The rates are similar in all coupons and a small reduction in surface diffusion rate occurs after the first 24 h as the diffusion process reaches its steady state.

3.2.2.2. Prediction of saturation time. The effects of hydrothermal ageing of composite laminates has seen substantial research interest and led to predictive methodologies such as that explored by Robin [1]. In the context of the durability of composite propellers, it is important to predict not only the time to saturation for an undamaged laminate but also the reduction in this duration as a result of impact damage. This is particularly important for propellers and other composite marine structures featuring a waterproof liner which prevents regular surface diffusion leaving water uptake to occur only at impact damage sites.

It is not useful to isolate and calculate the total amounts of relative water uptake due to damage-induced diffusion in this study as the residual strengths of damaged and undamaged laminates were all tested in the fully saturated state. However, change in diffusion rates due to impact damage can be used to estimate how much faster the impacted laminates reached saturation. Plots of relative mass changes in all laminates due to diffusion only are given in Fig. 12, allowing the prediction of saturation times in damaged laminates, similar to that performed on undamaged laminates using Fig. 8. Normalised saturation times were estimated from the intercept of each plot with the saturation level of 0.85 %. The results indicate small reductions in the saturation time due to 60 J and 90 J impacts of about 20 days for conical impacted laminates and 30 days for hemispherical impacted laminates. The greater reduction in saturation time due to hemispherical impacts may indicate that the larger surface areas exposed by delamination are more effective at accelerating diffusive mechanisms than the more severe intralaminar damage caused by conical impactors.

However, the difference, even for high energy impacts, is small and as advised earlier, caution is recommended when applying results for 60 °C ageing over such a long time period due to the potential for chemical changes to have a measurable effect on mass changes. Therefore, lower ageing temperatures are recommended to minimise errors associated with chemical changes in the laminate which may occur at elevated temperatures [1]. Larger specimens and larger sample sizes are also recommended to reduce errors associated with material and damage inconsistencies that are likely to affect estimated saturation times. The consistency of ageing water uptake in damaged laminates may also be improved by utilizing artificial damage, such as non-bonded laminate

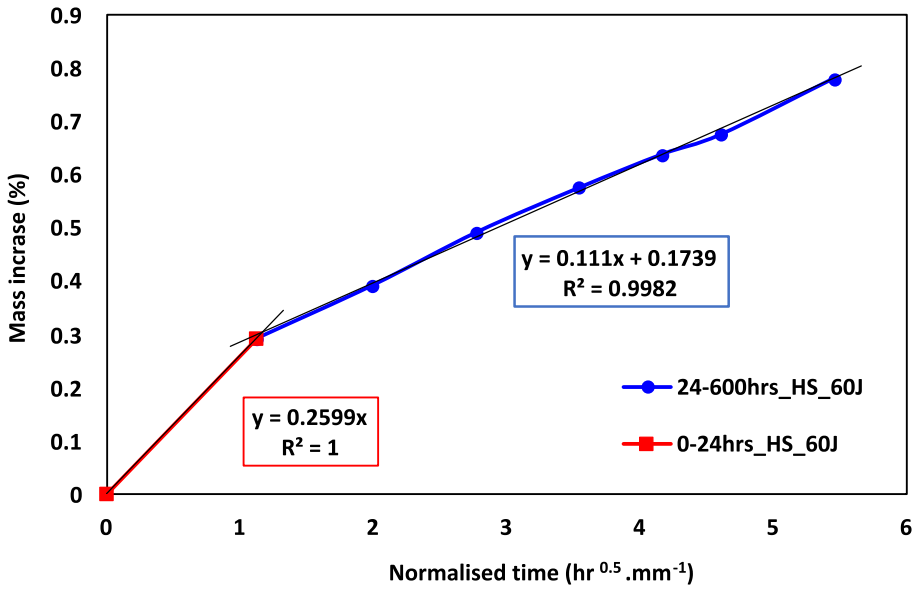

Fig. 10. Typical relative mass increase from 0 to 24 h (red squares) and from 24 to 600 h (blue circles) hydrothermal ageing. A maximum of 600 h was selected as the mass increase rate becomes non-linear beyond this time. Results for only the hemispherical, 60 J impacted coupon are plotted for clarity. Results for the remaining tests are given in Table 2.

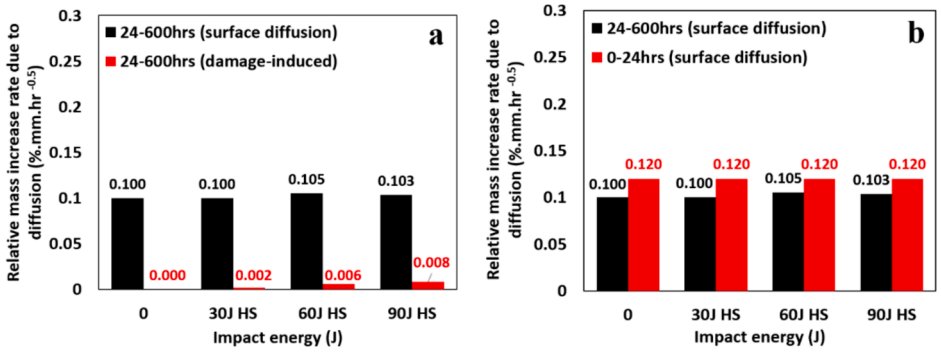

Fig. 11. The relative mass increase rates due to (a) surface (black) and damage-induced (red) diffusion in the 24–600 hr period and (b) surface diffusion alone (excluding effects of damage) for the first 24 hrs (red) and 24–600 hr period (black). Results are only shown for hemispherical impactors as conical impact results were similar.

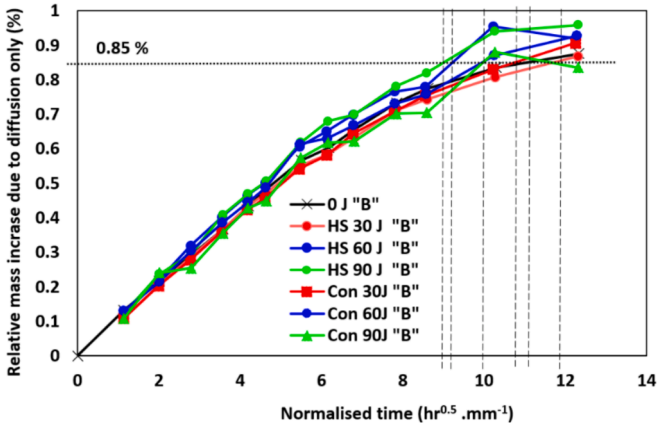

Fig. 12. Mass increase (%) via diffusion only during ageing at 60 °C of CF/Epoxy coupons impacted by a conical (Con) impactor and a hemispherical (HS) impactor showing the saturation level (0.85 %).

interfaces, rather than impact damage to verify assumptions concerning cavity filling and diffusion mechanisms.

3.2.2.3. Calculating the mass of water in damage cavities. In the context of a marine composite propeller, small imbalances in the rotational inertia can lead to significant vibration, noise and poor efficiency. Unlike diffusion in an undamaged propeller, which occurs globally, damage-induced water uptake occurs locally, and could thus large impacts could contribute to imbalances in the rotational inertia of composite marine propellers. Therefore, it is important to understand the mass associated with local water uptake after foreign body impact and correlate it with impact severity, determined by the impactor geometry and kinetic energy. Therefore, this study compares the impact energy level and impactor geometry with the mass of water uptake by cavity filling, the primary contributor to damage-induced weight gain.

This involves separating the water uptake due to capillary mechanisms from diffusive mechanisms by assuming a linear diffusion rate from the initial submersion time as observed in unimpacted laminates in Fig. 8. The diffusion-only water uptake rate (24–600 hrs in Fig. 10) is extended toward to the Y-axis, the initial submersion time. Y-intercept values, presented in Fig. 13, estimate the cavity water uptake as a

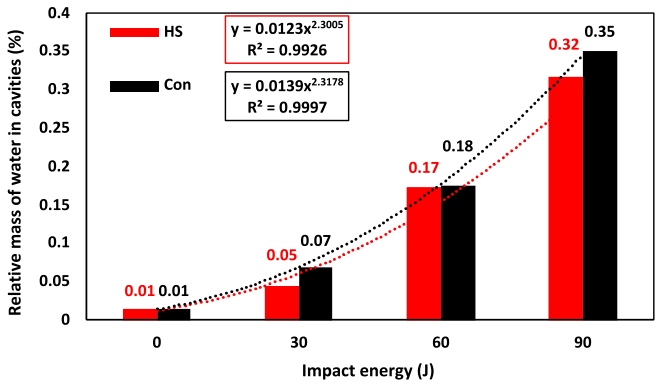

Fig. 13. Estimated relative mass gain (%) due to cavity-filling calculated from the y-intercept of trendlines parallel to the predicted diffusion-only linear region (24-600hrs) in Fig. 10.

percentage of laminate mass. A small amount of cavity water uptake shown for the unimpacted laminate may be the result of filling of air pockets which are exposed during cutting of the laminate. As expected, increased impact damage resulted in increased water uptake in cavities. The slightly greater uptake at conical impact sites may be the result of more exposed reinforcing fibres and fibre–matrix interfaces capable of capillary action. The rate at which the relative water uptake increases with impact energy is non-linear for the impact energy range tested. Curves have been fitted to hemispherical and conical impacted laminate results with reasonable correlation and could be used to predict the mass gain at the impact site for similar impacts in the given energy range. For consistency between laminates, the results are given in relative mass gain for specimens of approximately 100 g, however, a more useful formulation may be absolute mass gain, which is given in Table 3.

3.3. Residual strength

All of the impact-damaged coupons loaded in uniaxial compression failed via lateral cracking through the damage site in the middle of the specimen (LDM) failure while all the unimpacted coupons failed via lateral cracking near the top edge (LAT) [35]. The effects of impactor tip geometry, impact energy level and ageing on average residual compressive strengths are illustrated in Fig. 14a. Residual strength reduced with increased impact energy but showed almost no dependency on impactor geometry. The maximum difference in residual strengths attributable to the impactor tip shape alone was a 7 % reduction from hemispherical to conical impactor damage at 60 J.

Illustrated in the column graph in Fig. 14b is a 25 % reduction in the CAI strength of unimpacted CF/Epoxy laminates when hydrothermally aged for 4 months at 60 °C. This reduced to 8 % when impacted at 90 J by either impactor tip demonstrating the predominance of the effect of severe impact damage over ageing degradation and impactor geometry on residual strength. CAI strength reduced linearly from 0 J (no impact) to 30 J and 60 J impacts in both aged and unaged laminates. The reduction rate was approximately 1.9 MPa.J^{-1} for unaged laminates and 1.2 MPa.J^{-1} for aged laminates (Fig. 14a). As 90 J impacts experienced a change in damage modes, the resulting residual strength was similar to that of 60 J impacts for both aged and unaged laminates.

Ageing also had a significant effect on CAI failure strain (Fig. 16), with aged, pristine laminates failing at 15 % lower strains. This value reduced to about 5 % in 90 J impacted laminates. Stress–strain curves in Fig. 16 show load drops associated with progressive compression damage in 60 J and 90 J impacted coupons while appearing to show a primarily elastic response until failure in pristine and 30 J impacted coupons. The appearance of progressive damage during CAI tests showed a high sensitivity to the impact energy level but no apparent sensitivity to ageing or impactor geometry. Therefore, the sharper impactor used in this study provides no earlier failure warning for impacted laminates in compression than the standard hemispherical impactor. Despite reducing failure strength by up to 25 %, hydrothermal ageing also provides no early failure warnings making it both a significant and dangerous effect for composite propeller integrity.

4. Conclusions and recommendations

A study was conducted to assess the effect of impact damage on seawater ageing and post-impact ageing on the residual compressive strength of 4 mm thick, CF/Epoxy laminates. Laminates were subjected to a range of low velocity impacts and hydrothermal aged for 4 months in seawater at 60 °C before their residual compressive strength was compared with that of unaged laminates.

The unimpacted laminates reached saturation (0.85 % water mass uptake) after approximately 110 days in 60 °C seawater. While the

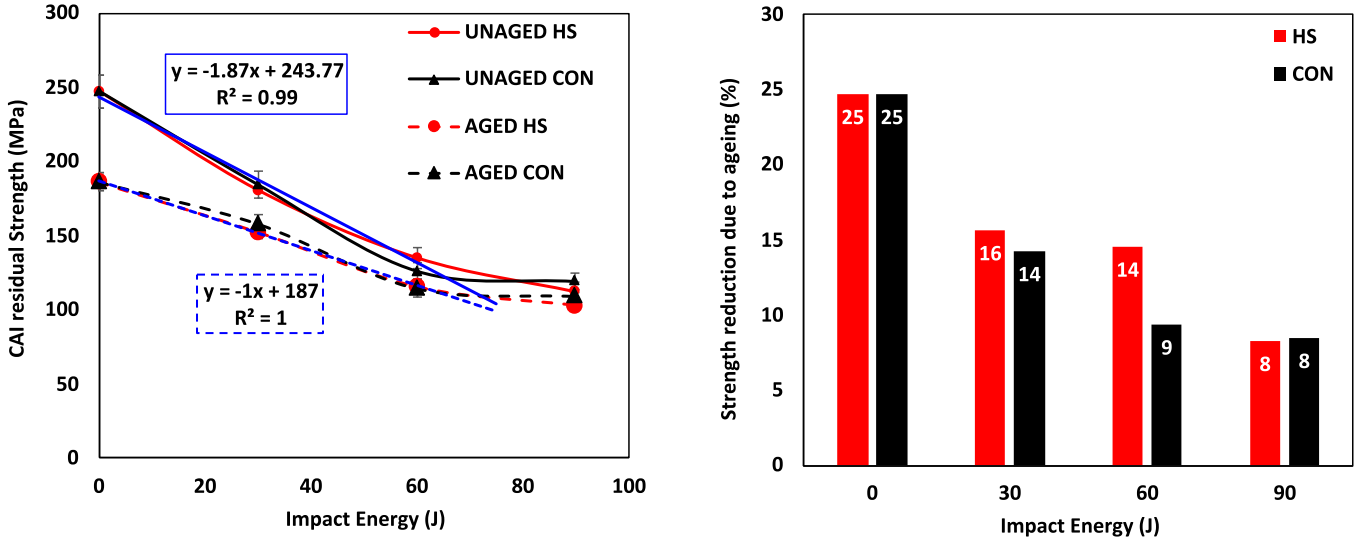

Fig. 14. (a) Change in CAI strength with impact energy for aged and unaged laminates impacted by hemispherical (HS) and conical (CON) impactors, and (b) residual strength reduction (%) due to ageing (difference between the CAI strength of aged and unaged coupons).

saturation time for 30 J impacted laminates was similar, 60 J and 90 J impacted laminates were saturated between 20 and 30 days earlier.

Larger mass increases in the impacted laminates are believed to be predominantly the result of damage cavity-filling at the damage site, occurring almost exclusively in the first 24 h of ageing and accounting for relative mass gains between 0.05 % and 0.3 % depending on the impact energy level. After the first 24 h of immersion, impact damage contributed only a small amount (0.008 %.mm.hr$^{-0.5}$) to the water uptake rate and is believed to be the result of the increase in surface area over which diffusive water uptake occurred.

The residual compressive strength of impacted then aged CF/Epoxy laminates was most sensitive to impact energy level, followed by ageing condition, followed by impactor shape. Impactor tip geometry had very little effect on hydrothermal ageing behaviour or residual strength for low energy impacts despite notably lower impact load carrying ability for high energy conical impacts. Ageing reduced the CAI strength of impacted coupons by a further 8 to 16 % depending on the damage level but the effect was greatest in pristine laminates at 25 %. For impacts up to 60 J, residual strength decreased with impact energy at rates of 1.9 MPa.J^{-1} for unaged laminates and 1.2 MPa.J^{-1} for aged laminates.

The methodology applied here offers a starting point for investigations aiming to predict the effect of impact damage on the saturation behaviour and residual strength of marine composite structures. Future work may include separate ageing-after-impact and compression-after-ageing-after-impact studies to accurately capture ageing behaviour and to investigate water uptake mechanisms individually. Further studies could also include shorter measurement intervals during the initial 24 h to further characterise capillary water uptake mechanisms. The same methodology may also be repeated with laminates coated in a waterproof liner to enable isolation of damage-induced diffusion and water uptake, a particularly dangerous situation where localised seawater ageing is unexpected and yet occurring in a dangerous location for residual strength retention.

CRediT authorship contribution statement

Rowan L. Caldwell: Writing – original draft, Methodology, Investigation, Formal analysis. **Peter Davies:** Writing – review & editing, Methodology, Conceptualization. **Mael Arhant:** Writing – review & editing, Methodology, Conceptualization. **B. Gangadhara Prusty:** Writing – review & editing, Supervision.

Declaration of competing interest

The authors declare the following financial interests/personal relationships which may be considered as potential competing interests: Rowan Caldwell reports financial support was provided by Defence Science and Technology Group. The other authors declare that they have no known competing financial interests or personal relationships that could have appeared to influence the work reported in this paper.

Data availability

Data will be made available on request.

Acknowledgements

Financial support from Defence Science and Technology Group (DSTG) is acknowledged. This project was conducted within the ARC Training Centre for Automated Manufacture of Advanced Composites (IC160100040). The lead author (R.L. Caldwell) acknowledges support from the Australian Government as an Australian Government Research Training Program Scholarship holder. The authors would like to thank Sebastien Le Jeune for manufacturing all composite laminates and guiding the process of ultrasonic C-scanning.

Appendix A

.

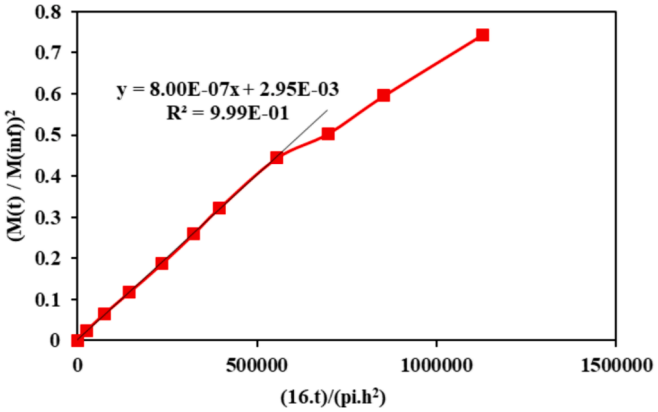

Fig. 15. Plot used to determine diffusivity using equation .

Appendix B

.

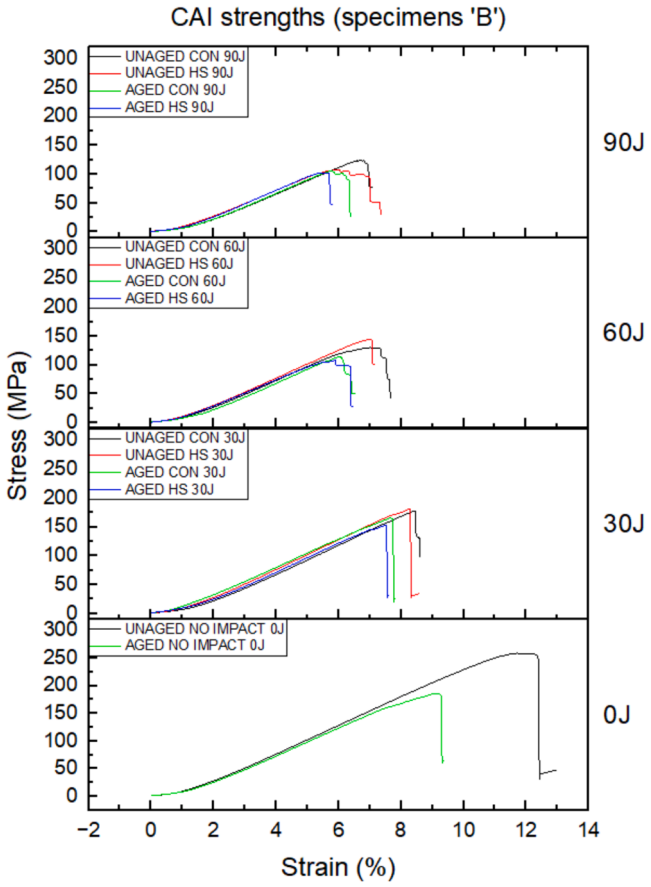

Fig. 16. Stressstrain results for CAI tests on aged and unaged coupons.

Appendix C

.

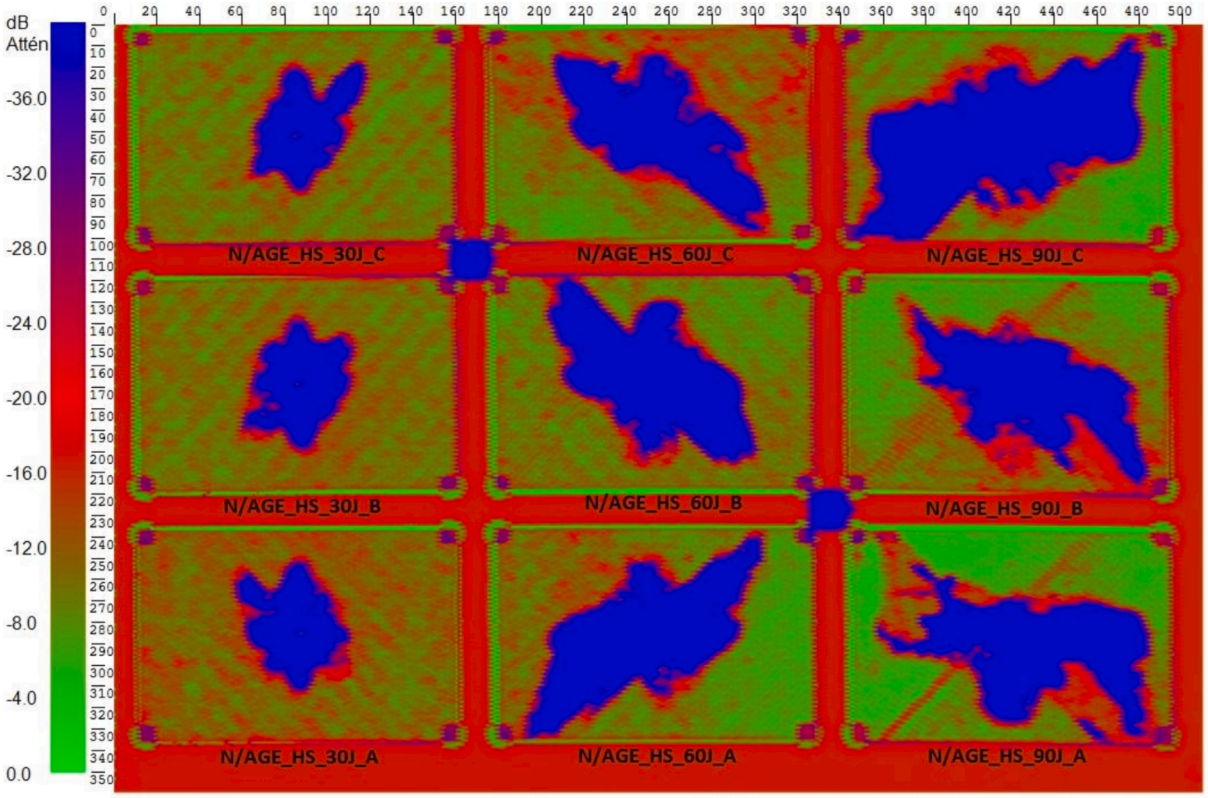

Fig. 17. Ultrasonic scans of un-aged, hemispherical tip impacted, CF/epoxy coupons showing damage areas in blue.

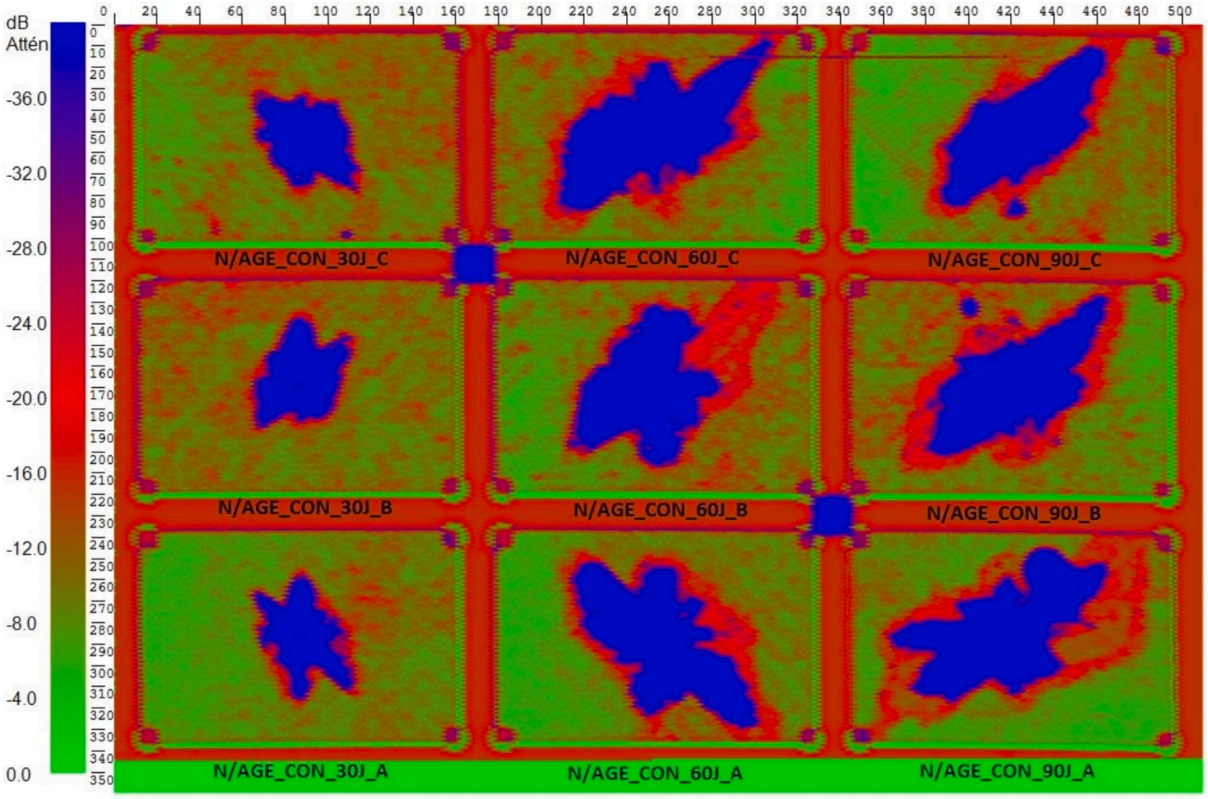

Fig. 18. Ultrasonic scans of un-aged, conical tip impacted, CF/epoxy coupons showing damage areas in blue.

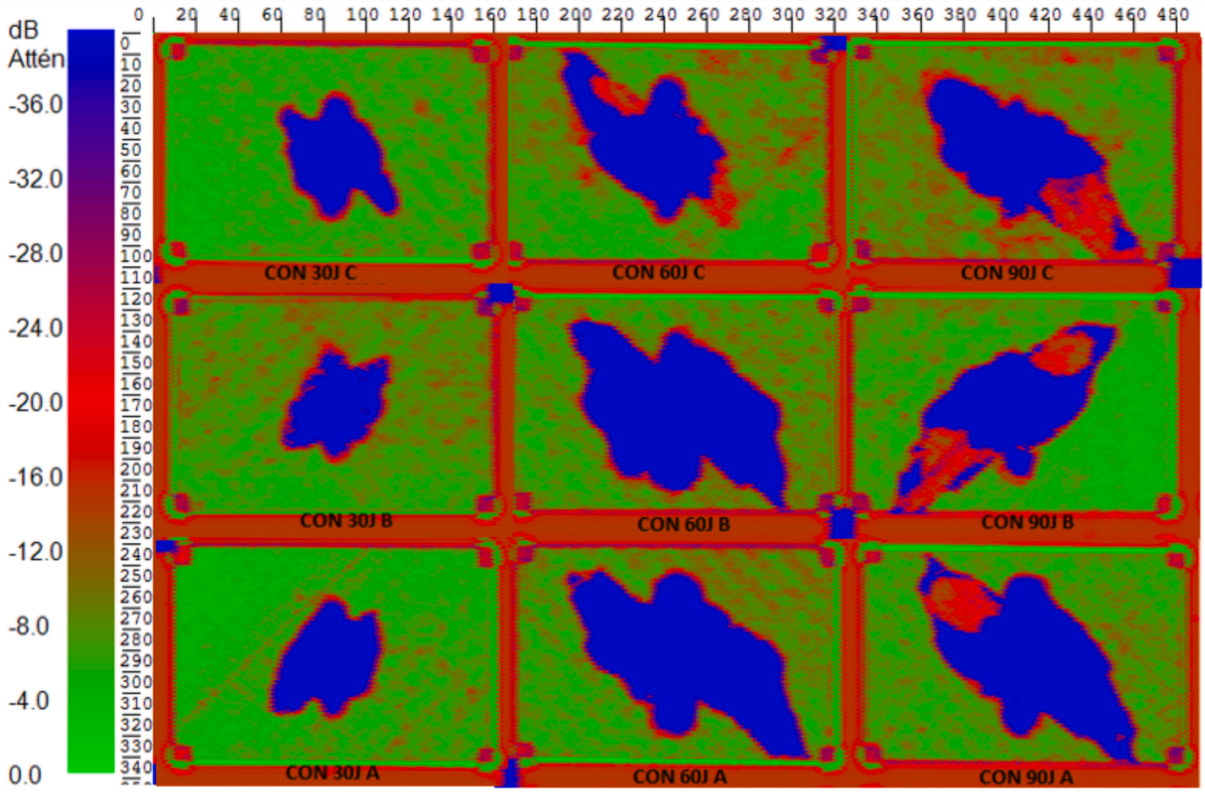

Fig. 19. Ultrasonic scans of conical tip impacted, CF/epoxy coupons prior to ageing showing damage areas in blue.

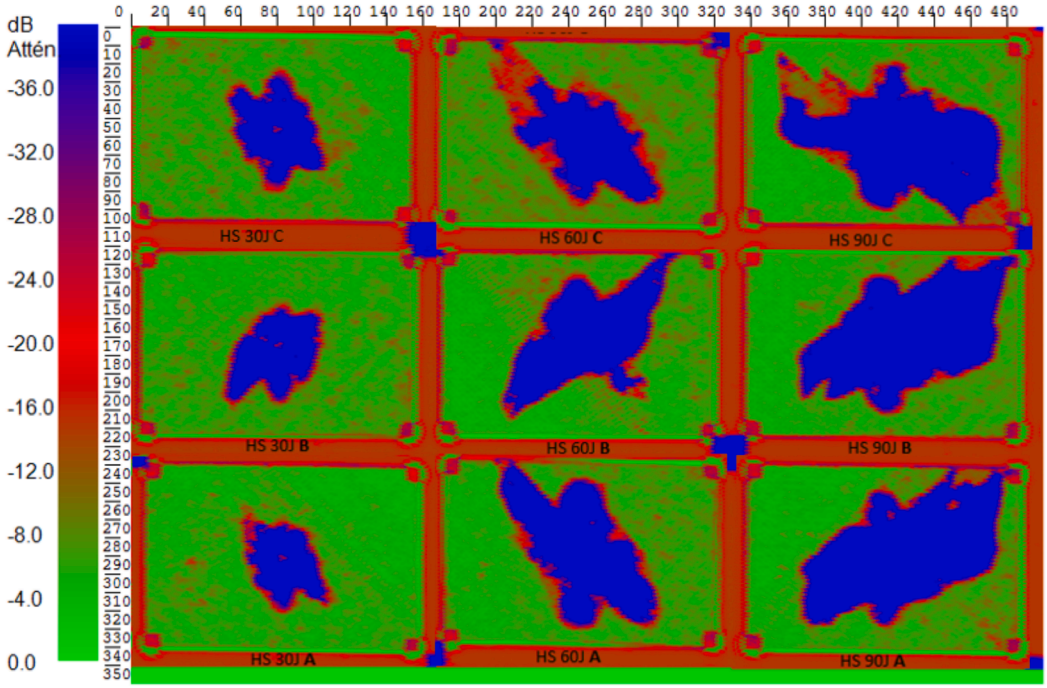

Fig. 20. Ultrasonic scans of hemispherical tip impacted, CF/epoxy coupons prior to ageing showing damage areas in blue.

Appendix D

Table 1
List of specimens and test conditions.

ID	Impactor diameter (mm)	Impact energy (J)	Ageing	Repeat
1	16.0 HS	0	age	1 of 3
2	16.0 HS	0	age	2 of 3
3	16.0 HS	0	age	3 of 3
4	16.0 HS	30	age	1 of 3
5	16.0 HS	30	age	2 of 3
6	16.0 HS	30	age	3 of 3
7	16.0 HS	60	age	1 of 3
8	16.0 HS	60	age	2 of 3
9	16.0 HS	60	age	3 of 3
10	16.0 HS	90	age	1 of 3
11	16.0 HS	90	age	2 of 3
12	16.0 HS	90	age	3 of 3
13	12.7 Conical	30	age	1 of 3
14	12.7 Conical	30	age	2 of 3
15	12.7 Conical	30	age	3 of 3
16	12.7 Conical	60	age	1 of 3
17	12.7 Conical	60	age	2 of 3
18	12.7 Conical	60	age	3 of 3
19	12.7 Conical	90	age	1 of 3
20	12.7 Conical	90	age	2 of 3
21	12.7 Conical	90	age	3 of 3
22	16.0 HS	0	no age	1 of 3
23	16.0 HS	0	no age	2 of 3
24	16.0 HS	0	no age	3 of 3
25	16.0 HS	30	no age	1 of 3
26	16.0 HS	30	no age	2 of 3
27	16.0 HS	30	no age	3 of 3
28	16.0 HS	60	no age	1 of 3
29	16.0 HS	60	no age	2 of 3
30	16.0 HS	60	no age	3 of 3
31	16.0 HS	90	no age	1 of 3
32	16.0 HS	90	no age	2 of 3
33	16.0 HS	90	no age	3 of 3
34	12.7 Conical	30	no age	1 of 3
35	12.7 Conical	30	no age	2 of 3
36	12.7 Conical	30	no age	3 of 3
37	12.7 Conical	60	no age	1 of 3
38	12.7 Conical	60	no age	2 of 3
39	12.7 Conical	60	no age	3 of 3
40	12.7 Conical	90	no age	1 of 3
41	12.7 Conical	90	no age	2 of 3
42	12.7 Conical	90	no age	3 of 3

Table 2
Relative mass increase rates (%.mm / $hr^{0.5}$) of all laminates in the first 24 h and from 24 to 600 h.

	Impact energy (J)	0	30		60		90	
	Impactor	None	HS	Con	HS	Con	HS	Con
Total wt% increase rates	First 24 h	0.12	0.14	0.16	0.26	0.27	0.39	0.40
	24 h – 600 h	0.10	0.10	0.10	0.11	0.11	0.11	0.10
Weight (%) increase rates due to damage only	First 24 h	0	0.02	0.04	0.14	0.15	0.27	0.29
	24 h – 600 h	0	0.0018	0.0025	0.0058	0.0027	0.0081	−0.0011

Table 3
Relative and absolute mass gains due to water uptake in cavities following impact damage.

Impactor	None	Con			HS		
Impact energy (J)	0	30	60	90	30	60	90
Relative mass gain (%)	0.014	0.069	0.175	0.351	0.045	0.174	0.317
Absolute mass gain (g)	0.014	0.070	0.177	0.345	0.045	0.170	0.319

References

[1] Robin A. Understanding the impact behavior and long-term durability of marine composites for propellers. 2023. PhD thesis, available at: https://theses.hal.science/tel-04401000.

[2] Cowie JM, Ferguson R. Physical aging studies in poly (vinylmethyl ether). I. Enthalpy relaxation as a function of aging temperature. Macromolecules 1989;22(5):2307–12.

[3] Starkova O, Buschhorn ST, Mannov E, Schulte K, Aniskevich A. Water transport in epoxy/MWCNT composites. Eur Polym J 2013;49(8):2138–48.

[4] Cabral-Fonseca S, Correia J, Rodrigues M, Branco F. Artificial accelerated ageing of GFRP pultruded profiles made of polyester and vinylester resins: characterisation of physical–chemical and mechanical damage. Strain 2012;48(2):162–73.

[5] Ben Daly H, Ben Brahim H, Hfaied N, Harchay M, Boukhili R. Investigation of water absorption in pultruded composites containing fillers and low profile additives. Polym Compos 2007;28(3):355–64.

[6] Ramirez F, Carlsson L, Acha B. Evaluation of water degradation of vinylester and epoxy matrix composites by single fiber and composite tests. J Mater Sci 2008;43:5230–42.
[7] Mourad A-H-I, Abdel-Magid BM, El-Maaddawy T, Grami ME. Effect of seawater and warm environment on glass/epoxy and glass/polyurethane composites. Appl Compos Mater 2010;17:557–73.
[8] Islam F, Caldwell R, Phillips AW, St John NA, Prusty BG. A review of relevant impact behaviour for improved durability of marine composite propellers. Composites Part C: Open Access; 2022. p. 100251.
[9] Andrew JJ, Srinivasan SM, Arockiarajan A, Dhakal HN. Parameters influencing the impact response of fiber-reinforced polymer matrix composite materials: a critical review. Compos Struct 2019;224:111007.
[10] Chen C. Investigation of environmental effects on impact damage tolerance of composite laminates. Institut Clément Ader; 2015.
[11] Dhakal HN, MacMullen J, Zhang Z. Moisture measurement and effects on properties of marine composites. Marine applications of advanced fibre-reinforced composites: Elsevier; 2016. p. 103–24.
[12] Fernandes O, Dutta J, Pai Y. Effect of various factors and hygrothermal ageing environment on the low velocity impact response of fibre reinforced polymer composites-a comprehensive review. Cogent Engineering 2023;10(1):2247228.
[13] Liao K, Schultheisz C, Hunston DL. Effects of environmental aging on the properties of pultruded GFRP. Compos B Eng: Engineering 1999;30(5):485–93.
[14] Atas C, Dogan A. An experimental investigation on the repeated impact response of glass/epoxy composites subjected to thermal ageing. Compos B Eng 2015;75:127–34.
[15] Ahmad F, Hong J-W, Choi HS, Park MK. Hygro effects on the low-velocity impact behavior of unidirectional CFRP composite plates for aircraft applications. Compos Struct 2016;135:276–85.
[16] Berketis K, Tzetzis D, Hogg P. The influence of long term water immersion ageing on impact damage behaviour and residual compression strength of glass fibre reinforced polymer (GFRP). Mater Des 2008;29(7):1300–10.
[17] Strait LH, Karasek ML, Amateau MF. Effects of seawater immersion on the impact resistance of glass fiber reinforced epoxy composites. J Compos Mater 1992;26(14):2118–33.
[18] Li G, Pang SS, Helms JE, Ibekwe SI. Low velocity impact response of GFRP laminates subjected to cycling moistures. Polym Compos 2000;21(5):686–95.
[19] Kootsookos A, Mouritz AP. Seawater durability of glass-and carbon-polymer composites. Compos Sci Technol 2004;64(10–11):1503–11.
[20] Boukhoulda F, Guillaumat L, Lataillade J, Adda-Bedia E, Lousdad A. Aging-impact coupling based analysis upon glass/polyester composite material in hygrothermal environment. Mater Des 2011;32(7):4080–7.
[21] Vieille B, Aucher J, Taleb L. Comparative study on the behavior of woven-ply reinforced thermoplastic or thermosetting laminates under severe environmental conditions. Mater Des 2012;35:707–19.
[22] Imielińska K, Guillaumat L. The effect of water immersion ageing on low-velocity impact behaviour of woven aramid–glass fibre/epoxy composites. Compos Sci Technol 2004;64(13–14):2271–8.
[23] Kimpara I, Saito H. Post-impact fatigue behavior of woven and knitted fabric CFRP laminates for marine use. Major Accomplishments in Composite Materials and Sandwich Structures 2009:113–32.
[24] Dale M, Acha BA, Carlsson LA. Low velocity impact and compression after impact characterization of woven carbon/vinylester at dry and water saturated conditions. Compos Struct 2012;94(5):1582–9.
[25] Abdel-Magid B, Ziaee S, Gass K, Schneider M. The combined effects of load, moisture and temperature on the properties of E-glass/epoxy composites. Compos Struct 2005;71(3–4):320–6.
[26] Deniz ME, Karakuzu R. Seawater effect on impact behavior of glass–epoxy composite pipes. Compos B Eng 2012;43(3):1130–8.
[27] Stober EJ, Seferis JC, Keenan JD. Characterization and exposure of polyetheretherketone (PEEK) to fluid environments. Polymer 1984;25(12):1845–52.
[28] Choqueuse D, Davies P, Mazeas F, Baizeau R. Aging of composites in water: comparison of five materials in terms of absorption kinetics and evolution of mechanical properties. High Temperature and Environmental Effects on Polymeric Composites: 2nd Volume: ASTM International; 1997.
[29] Selzer R, Friedrich K. Mechanical properties and failure behaviour of carbon fibre-reinforced polymer composites under the influence of moisture. Compos A Appl Sci Manuf 1997;28(6):595–604.
[30] Loos AC, Springer GS, Sanders BA, Tung RW. Moisture absorption of polyester-E glass composites. J Compos Mater 1980;14(2):142–54.
[31] Zhang A, Lu H, Zhang D. Effects of voids on residual tensile strength after impact of hygrothermal conditioned CFRP laminates. Compos Struct 2013;95:322–7.
[32] Rubio-González C, Hernández-Santos M, José-Trujillo E, Rodríguez-González JA. Effect of seawater aging on impact behavior of glass fiber/epoxy laminates with drilled holes. J Compos Mater 2022;56(10):1481–93.
[33] Le Guen-Geffroy A. Marine ageing and fatigue of carbon/epoxy composite propeller blades. Université de Bretagne occidentale-Brest; 2019.
[34] Crank J. The mathematics of diffusion. Oxford University Press; 1979.
[35] International A. Standard Test Method for Measuring the Damage Resistance of a Fiber-Reinforced Polymer Matrix Composite to a Drop-Weight Impact Event. 2017.